Available online at www.sciencedirect.com
ScienceDirect
Journal of Power Sources 160 (2006) 194–201
JOURNAL OF POWER SOURCES
www.elsevier.com/locate/jpowsour

PEM FC with improved water management

Alexander Kraytsberg, Yair Ein-Eli *

Department of Materials Engineering, Technion-Israel Institute of Technology, Haifa 32000, Israel

Received 26 July 2005; received in revised form 14 November 2005; accepted 21 December 2005
Available online 13 February 2006

Abstract

Water management problems of proton exchange membrane (PEM)-based H_2/O_2 and H_2/air fuel cell systems (PEM FC) are considered. It is demonstrated that PEM FC performance and efficiency are strongly influenced by water transport phenomena. A new water management scheme, based on anode side water removal, is suggested. It is shown that such a scheme may be very efficient if implementing cathode modified by oxygen permeable liquid perfluorocarbones. Possible efficiency of such a PEM FC is estimated using literature-based parameters of existing practical PEM FC.

Keywords: PEM fuel cell; Mathematical model; Water management

1. Introduction

The proton exchange membrane H_2/O_2 and H_2/air fuel cell systems (PEM FC) have high efficiency, are simple in design and operation, and also are environmentally friendly. These features make them a viable power source, particularly for vehicles. However, their performance and efficiency need to be improved in order for PEM FC systems to be cost effective for practical use. Water transport phenomena have a strong impact on operation efficiency and power output of PEM FC. Thus, an improvement of water management scheme is of considerable practical interest.

Fig. 1 schematically shows processes of water generation and transfer inside PEM FC unit. During operation, cathode water contents depend on the balance of water generation rate at the cathode by the oxygen reduction reaction, water delivery by electro-osmotic drag, and the rate of water removal from the cathode by back-diffusion to the anode and water removal with oxygen/air and hydrogen flows. This last process comprises of water vapor diffusion, convection and also capillary transport of liquid water through the porous cathode and anode backing layers. Anode water content depends on balance of water delivery by back-diffusion from cathode side through PEM, osmotic drag flux and water diffusion from (or to) fuel gas stream. Also, PEM has to contain a certain amount of water to maintain a proper conductivity, i.e. PEM FC may be considered as self-humidifying only when in a high current mode, whereas the membrane water content is mainly governed by fuel and oxidant gas stream humidity when the current is below some particular level. It may be suggested that performance of a fuel cell may be improved if the humidity of the fuel hydrogen varies in consistency of the fuel cell load but the detailed consideration of optimal PEM FC operation modes is out of the scope of this work.

Total PEM FC water balance depends on the fuel cell current and water content of fuel and oxidant gas stream. Finally, in case of a steady state operation conditions, all cathode generated water has to be removed by these gas streams. When current density exceeds a certain level, the water delivery (by electro-osmotic drag and the oxygen-reduction reaction) exceeds the water removal from the cathode catalyst and/or backing layers. In such case, water accumulation takes place and electrode flooding occurs, the rate of oxygen transport to the catalyst sites in the cathode is greatly reduced, and the electrode reaction becomes mass-transport-limited, giving rise to the rapid increase in the cathode overvoltage, and a considerable decrease in the FC power. In the same way, when water delivery by back-diffusion from the cathode side to the anode exceeds electro-osmotic drag and water removal by fuel gas stream, anode flooding occurs.

* Corresponding author.
E-mail address: eineli@tx.technion.ac.il (Y. Ein-Eli).

0378-7753/$ – see front matter © 2006 Elsevier B.V. All rights reserved.
doi:10.1016/j.jpowsour.2005.12.074

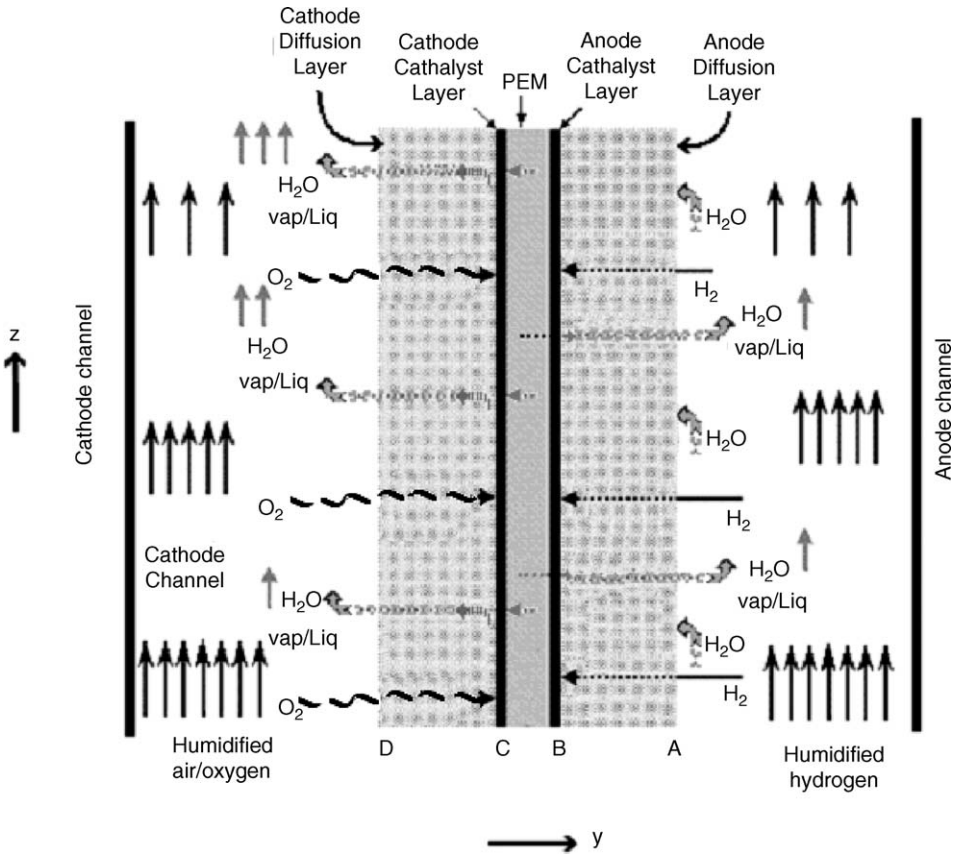

Fig. 1. Schematic representation of water transport processes in PEM FC.

Practical PEM FC design is represented in Fig. 2. Fuel cell assembly (MEA) comprises of two (cathode and anode) gas diffusion layers (GDLs), cathode catalyst layer, anode catalyst layer and PEM; this assembly is sandwiched between two bipolar conductive plates. These plates are closely attached to GDLs and have grooves for gas to flow. Gas delivery and water removal take place through these grooves, which are machined into the plates' body.

2. General assumptions

Generally, water concentration in a real PEM FC unit is a three-dimensional function (this fact is illustrated in Fig. 3). There is water content gradient along the direction *Y* (transversal to the membrane) and also along the direction *X*, which is parallel to the membrane plane but transversal to the groove.

Whereas PEM and cathode water content may be assumed being approximately constant along axis *X* over the groove (area ① in Fig. 3), the content may be substantially variable along *X*-coordinate in the areas over the bipolar plate shoulder (area ② in Fig. 3). Water content of a membrane, a catalyst layer and a GDL vary along the groove. Beginning from the gas inlet, water gradually saturates the gas in a groove, as the gas moves along the groove from inlet to outlet. This gives the third argument

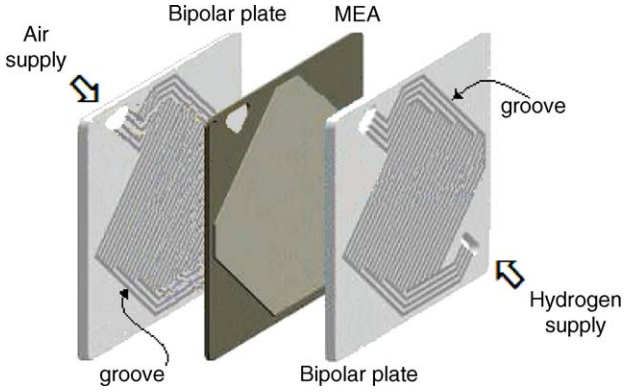

Fig. 2. Practical design of PEM FC unit.

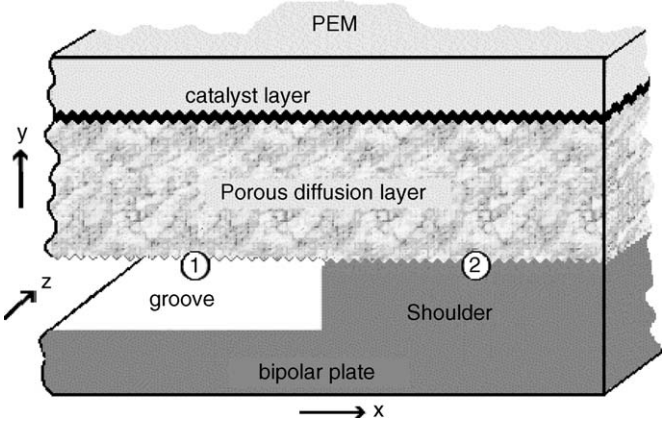

Fig. 3. Cross-sectional view of PEM FC unit.

(axis Z in Fig. 3), which is the distance from gas inlet along the gas groove. Summing up, water content of the PEM FC has to be represented as the function of the three aforementioned independent variables—x, y and z: $\mathbf{W}_{\mathrm{PEM\ FC}} = \mathbf{W}(x, y, z)$.

Simplifying the case, it is assumed in the current work that the function $\mathbf{W}(x, y, z)$ is a function with separated variables, and thus may be written as: $\mathbf{W}(x, y, z) = \Im(x) \times \Re(y) \times \aleph(z)$. It is understandable that water and gas transport rates strongly depends on design parameters (specific bipolar plate dimensions, gas flow rate, etc.) in the areas along the bipolar plate groove and over the bipolar plate shoulder. This makes reasonable to assume that in the above representation functions $\Im(x)$ and $\aleph(z)$ may be substituted with their average values $\langle\Im(x)\rangle$ and $\langle\aleph(z)\rangle$, which results in reduction of three-dimensional function $\mathbf{W}(x, y, z)$ to a one-dimensional function $\mathfrak{W}(y) : \mathfrak{W}(y) = \langle\Im(x)\rangle \times \langle\aleph(z)\rangle \times \Re(y)$. The approach, which based on the consideration of one-dimensional water distribution function $\Re(y)$, will be thereafter generally adopted.

3. Assessment of flooding limits of standard PEM FC unit

As it has been discussed above, the purpose of water management is to maintain the conductivity of PEM, whatever the operation mode is, and to alleviate electrode flooding. The first goal is achieved by humidification of gas streams. It was demonstrated [1,2] that Nafion™ PEM conductivity reaches saturation if Nafion™ membrane is equilibrated with water vapors with RH > 50%:

$$\frac{1}{2}C_{\mathrm{sat}}^{\mathrm{water}} \leq C_{\mathrm{Channel}}^{\mathrm{water}}; \tag{1}$$

where $C_{\mathrm{sat}}^{\mathrm{water}}$ is saturated water vapor concentration and $C_{\mathrm{Channel}}^{\mathrm{water}}$ is a water concentration in a gas channel.

On the other hand, the challenge is in alleviating flooding when PEM FC is in a high current operational mode (just for example: water production associated with a current of 1 A cm^{-2} is sufficient to completely hydrate a dry 50 mm thick Nafion™ 112 membrane in roughly 10 s [3]). Water generates at the PEM–cathode interface (surface C in Fig. 1) of the PEM FC; the rate of water generation $J_{\mathrm{Faraday}}^{\mathrm{water}}$ is given by expression (2):

$$J_{\mathrm{Faraday}}^{\mathrm{water}} = M^{\mathrm{water}}\frac{j_{\mathrm{FC}}}{2F}; \tag{2}$$

where M^{water} is molecular weight of water, j_{FC} the current density through the PEM and F is Faraday number.

All generated water has to be removed from FC by gas fluxes in anode ($J_{\mathrm{AChannel}}^{\mathrm{water}}$) and cathode ($\hat{J}_{\mathrm{CChannel}}^{\mathrm{water}}$) channels if the cell is in a steady state. The water removing ensues by water vapor transport through electrode/PEM interfaces (surfaces C and B in Fig. 1) toward GDLs, then the water transport goes on across GDLs toward gas channels and then it take place through GDL/gas channel interfaces (surfaces A and D in Fig. 1) into the gas streams. Flooding starts when the water vapor concentration inside GDLs and/or electrode catalyst layers exceeds this value for saturated water vapors; although water transport inside GDL continues even if water condensation starts (liquid water transport is driven by wicking force inside GDL), in this case water droplets gradually block GDL's and catalyst layer's pores and thus hinder oxygen transport toward catalyst surface and at least 20% of electrode volume should be available for gas transport to maintain fairly high current density [4,5].

Assuming that there in no liquid formation inside GDLs, inside electrode catalyst layers and onto their boundaries, diffusion may be considered as the main mechanism for water transport through the porous GDL (convection is considered to be negligible due to the small GDL pore size). In this case, the water vapor flux toward the anode GDL/channel interface ($J_{\mathrm{GDL}}^{\mathrm{water}}$) and the water vapor flux toward cathode GDL/channel interface ($\hat{J}_{\mathrm{GDL}}^{\mathrm{water}}$) are governed by Eqs. (3) and (3.1) below [6]:

$$J_{\mathrm{GDL}}^{\mathrm{water}} = D_{\mathrm{hydrogen}}^{\mathrm{water}}\varepsilon\frac{C_{\mathrm{B}}^{\mathrm{water}} - C_{\mathrm{A}}^{\mathrm{water}}}{\delta_{\mathrm{GDL}}}, \tag{3}$$

$$\hat{J}_{\mathrm{GDL}}^{\mathrm{water}} = D_{\mathrm{air}}^{\mathrm{water}}\hat{\varepsilon}\frac{C_{\mathrm{D}}^{\mathrm{water}} - C_{\mathrm{C}}^{\mathrm{water}}}{\hat{\delta}_{\mathrm{GDL}}}; \tag{3.1}$$

here $C_{\mathrm{B}}^{\mathrm{water}}$ is water concentration on B surface, $C_{\mathrm{A}}^{\mathrm{water}}$ the water concentration on A surface, $C_{\mathrm{C}}^{\mathrm{water}}$ the water concentration on C surface, $C_{\mathrm{D}}^{\mathrm{water}}$ the water concentration on D surface, δ_{GDL} the anode GDL thickness, $\hat{\delta}_{\mathrm{GDL}}$ the cathode GDL thickness, ε the anode GDL porosity, $\hat{\varepsilon}$ the cathode GDL porosity, $D_{\mathrm{hydrogen}}^{\mathrm{water}}$ the diffusion coefficient of water vapors into the hydrogen-filled anode GDL and $D_{\mathrm{air}}^{\mathrm{water}}$ is a diffusion coefficient of water vapors into the air-filled cathode GDL media (a linear approximation of $C^{\mathrm{water}}(y)$ function is assumed).

Being delivered to the GDL/gas channel interfaces A and D, water vapors are transported into the gas streams by convective process, which is governed by Eqs. (4) and (4.1) [7]:

$$J_{\mathrm{AChannel}}^{\mathrm{water}} = h_{\mathrm{m}}(C_{\mathrm{A}}^{\mathrm{water}} - \langle C_{\mathrm{AChannel}}^{\mathrm{water}}\rangle) \tag{4}$$

$$\hat{J}_{\mathrm{CChannel}}^{\mathrm{water}} = \hat{h}_{\mathrm{m}}(\langle\hat{C}_{\mathrm{CChannel}}^{\mathrm{water}}\rangle - C_{\mathrm{D}}^{\mathrm{water}}) \tag{4.1}$$

where $J_{\mathrm{AChannel}}^{\mathrm{water}}$ is a water vapor flux across surface A, $\hat{J}_{\mathrm{CChannel}}^{\mathrm{water}}$ the water vapor flux across surface D, $\langle C_{\mathrm{AChannel}}^{\mathrm{water}}\rangle$ the average water vapor concentration in the anode gas channel, $\langle\hat{C}_{\mathrm{CChannel}}^{\mathrm{water}}\rangle$ the average water vapor concentration in the cathode gas channel and h_{m} and $\hat{h}_{\mathrm{m}}$ are mass transfer coefficients between the anode GDL and anode gas channel and cathode GDL and cathode gas channel, respectively.

Coefficients h_{m} and $\hat{h}_{\mathrm{m}}$ may be estimated considering that mass transfer in a fully developed laminar flow through a parallel-plate channel with a constant mass flux applied at one surface and no-flux applied at the other. In this situation, the dimensionless mass transfer coefficient (Sherwood number) is

$$\underline{Sh} \cong \frac{\dot{h}_{\mathrm{m}}\Delta_{\mathrm{Channel}}}{D_{\mathrm{gas}}^{\mathrm{water}}} = 2.7; \tag{5}$$

where $\Delta_{\mathrm{Channel}}$ is a gas channel opening, $\dot{h}_{\mathrm{m}}$ mass transfer coefficient and $D_{\mathrm{gas}}^{\mathrm{water}}$ is a diffusion coefficient of water into a gas, which fills the channel [6].

In this case, the h_{m} and $\hat{h}_{\mathrm{m}}$ may be determined as

$$h_{\mathrm{m}} \cong 2.7\frac{D_{\mathrm{hydrogen}}^{\mathrm{water}}}{\Delta_{\mathrm{AChannel}}} \tag{6}$$

$$\hat{h}_{\mathrm{m}} \cong 2.7\frac{D_{\mathrm{air}}^{\mathrm{water}}}{\hat{\Delta}_{\mathrm{CChannel}}} \tag{6.1}$$

where $\Delta_{\mathrm{AChannel}}$ and $\hat{\Delta}_{\mathrm{CChannel}}$ are, respectively, anode and cathode channel openings.

Taking in consideration, that there is no accumulation and/or water leakage at surfaces A and D, the following relations can be presented:

$$j_{\mathrm{AChannel}}^{\mathrm{water}} = j_{\mathrm{GDL}}^{\mathrm{water}} \tag{7}$$

$$\hat{\jmath}_{\mathrm{CChannel}}^{\mathrm{water}} = \hat{\jmath}_{\mathrm{GDL}}^{\mathrm{water}} \tag{7.1}$$

Now, the water balance at cathode–PEM interface (C) is to be considered. First, water generation takes place in the cathode catalyst layer, according to Eq. (2). Second, there is an electro-osmotic water flux toward the border. The flux exists because of the hydration of protons, which move from anode toward cathode; water molecules, which are trapped inside their hydrate shell, move along with these protons. The rate of electro-osmotic water delivery is given by expression (8) below (j_{FC} is positive if there is an oxidation at the anode):

$$J_{\mathrm{EOsmos}}^{\mathrm{water}} = -M^{\mathrm{water}}\frac{\alpha j_{\mathrm{FC}}}{F} \tag{8}$$

where α is a transference number.

Also, there is a water diffusion flux from C toward surface B through PEM (see Fig. 1):

$$J_{\mathrm{PEM}}^{\mathrm{water}} = D_{\mathrm{PEM}}^{\mathrm{water}}\frac{C_{\mathrm{C}}^{\mathrm{water}} - C_{\mathrm{B}}^{\mathrm{water}}}{\delta_{\mathrm{PEM}}}; \tag{9}$$

where $C_{\mathrm{C}}^{\mathrm{water}}$ is a water concentration on the C surface, δ_{spe} the PEM thickness and $D_{\mathrm{PEM}}^{\mathrm{water}}$ is a water-in-PEM diffusion coefficient (a linear approximation of $C^{\mathrm{water}}(y)$ is assumed).

The resultant water flux toward surface C is given by expression (10) below:

$$J_{\mathrm{C}}^{\mathrm{water}} = -J_{\mathrm{PEM}}^{\mathrm{water}} + \hat{\jmath}_{\mathrm{GDL}}^{\mathrm{water}} - J_{\mathrm{EOsmos}}^{\mathrm{water}} + J_{\mathrm{Faraday}}^{\mathrm{water}} \tag{10}$$

Assuming that the FC unit is working in a steady state mode, there is no water accumulation or depletion anywhere in the FC unit, and all water generated in the unit is removed trough cathode and anode gas channels. In such instance relation (11) has to be kept:

$$\hat{\jmath}_{\mathrm{CChannel}}^{\mathrm{water}} + J_{\mathrm{Faraday}}^{\mathrm{water}} = J_{\mathrm{AChannel}}^{\mathrm{water}} \tag{11}$$

Combining expressions (2)–(4.1), (7)–(10) and (11) results in equation system (12.1)–(12.4), which describes water transport in FC unit:

$$\frac{M^{\mathrm{water}}}{F}\left(\frac{1+2\alpha}{2}\right) j_{\mathrm{FC}} = D_{\mathrm{PEM}}^{\mathrm{water}}\frac{C_{\mathrm{C}}^{\mathrm{water}} - C_{\mathrm{B}}^{\mathrm{water}}}{\delta_{\mathrm{PEM}}} + D_{\mathrm{air}}^{\mathrm{water}}\hat{\varepsilon}\frac{C_{\mathrm{C}}^{\mathrm{water}} - C_{\mathrm{D}}^{\mathrm{water}}}{\hat{\delta}_{\mathrm{GDL}}} \tag{12.1}$$

$$\hat{\jmath}_{\mathrm{GDL}}^{\mathrm{water}} = D_{\mathrm{air}}^{\mathrm{water}}\hat{\varepsilon}\frac{C_{\mathrm{D}}^{\mathrm{water}} - C_{\mathrm{C}}^{\mathrm{water}}}{\hat{\delta}_{\mathrm{GDL}}} = \hat{h}_{\mathrm{m}}(\langle\hat{C}_{\mathrm{CChannel}}^{\mathrm{water}}\rangle - C_{\mathrm{D}}^{\mathrm{water}}) = \hat{\jmath}_{\mathrm{CChannel}}^{\mathrm{water}} \tag{12.2}$$

$$J_{\mathrm{GDL}}^{\mathrm{water}} = D_{\mathrm{hydrogen}}^{\mathrm{water}}\varepsilon\frac{C_{\mathrm{B}}^{\mathrm{water}} - C_{\mathrm{A}}^{\mathrm{water}}}{\delta_{\mathrm{GDL}}} = h_{\mathrm{m}}(C_{\mathrm{A}}^{\mathrm{water}} - \langle C_{\mathrm{AChannel}}^{\mathrm{water}}\rangle) = J_{\mathrm{AChannel}}^{\mathrm{water}} \tag{12.3}$$

$$\frac{M^{\mathrm{water}}}{2F} j_{\mathrm{FC}} = h_{\mathrm{m}}(C_{\mathrm{A}}^{\mathrm{water}} - \langle C_{\mathrm{AChannel}}^{\mathrm{water}}\rangle) + \hat{h}_{\mathrm{m}}(C_{\mathrm{D}}^{\mathrm{water}} - \langle C_{\mathrm{CChannel}}^{\mathrm{water}}\rangle) \tag{12.4}$$

Different numeric values for diffusion coefficients, mass transfer coefficients and transference number are presented in a considerable amount of articles. The particular numbers depend on the conditions, used materials, measurement methods, etc. The purpose of our further numerical calculations is just to compare efficiency of a classic FC water management model with efficiency of a modified water management design (a brief sketch of this design will be presented later on). Because of this goal it seems reasonable instead of launching a critical review of this literature just to use the same values for estimating an efficiency of both water management models. It is assumed, in further calculations, that $\hat{\varepsilon} = \varepsilon$, $\delta_{\mathrm{GDL}} = \hat{\delta}_{\mathrm{GDL}}$ (which means that cathode and anode GDLs are identical—same material, porosity, thickness, etc.), $\Delta_{\mathrm{AChannel}} = \hat{\Delta}_{\mathrm{CChannel}}$, $\langle C_{\mathrm{AChannel}}^{\mathrm{water}}\rangle = \langle\hat{C}_{\mathrm{CChannel}}^{\mathrm{water}}\rangle = (1/2)C_{\mathrm{sat}}^{\mathrm{water}}$, and that PEM FC unit is working at room temperature; also, the following numeric values are assumed:

(i) $D_{\mathrm{PEM}}^{\mathrm{water}}$ depends on the water content for literature data vary from $5\times10^{-10}\,\mathrm{m^2\,s^{-1}}$ [7] to $1.5\times10^{-10}\,\mathrm{m^2\,s^{-1}}$ [8] for different conditions and also for different Nafion$^{\mathrm{TM}}$s; below $D_{\mathrm{PEM}}^{\mathrm{water}}$ is assumed to be $1.5\times10^{-10}\,\mathrm{m^2\,s^{-1}}$ in case of commercially available fully hydrated Nafion$^{\mathrm{TM}}$ 117 PEM.
(ii) α: different electro-osmotic drag coefficient α values may be found in literature; it is assumed to be ∼1 for Nafion$^{\mathrm{TM}}$ 117 PEM [9].
(iii) δ_{PEM} depends on the specific SPE membrane brand, which is used. In case of Nafion$^{\mathrm{TM}}$ 112, $\delta_{\mathrm{PEM}} = 5\times10^{-5}\,\mathrm{m}$ [10].
(iv) $C_{\mathrm{sat}}^{\mathrm{water}}$ is assumed to be $23.05\times10^{-3}\,\mathrm{kg\,m^{-3}}$ (at 25°), and thus $\langle C_{\mathrm{CChannel}}^{\mathrm{water}}\rangle$; $\langle C_{\mathrm{AChannel}}^{\mathrm{water}}\rangle \geq \frac{1}{2}C_{\mathrm{sat}}^{\mathrm{water}} = 11.53\times10^{-3}\,\mathrm{kg\,m^{-3}}$.
(v) $\delta_{\mathrm{GDL}} = \hat{\delta}_{\mathrm{GDL}}$, and both are assumed to be $5\times10^{-4}\,\mathrm{m}$ [11].
(vi) $\varepsilon = \hat{\varepsilon}$, and both are assumed to be 0.3 [6].
(vii) $D_{\mathrm{hydrogen}}^{\mathrm{water}}$ is assumed to be $0.90\times10^{-4}\,\mathrm{m^2\,s^{-1}}$ [12].
(viii) $D_{\mathrm{air}}^{\mathrm{water}}$ is assumed to be $0.26\times10^{-4}\,\mathrm{m^2\,s^{-1}}$ [14].
(ix) $\Delta_{\mathrm{AChannel}} = \hat{\Delta}_{\mathrm{CChannel}}$ is assumed to be $7\times10^{-4}\,\mathrm{m}$ [6]; $M^{\mathrm{water}} = 18$, $N^{\mathrm{water}} = 3.36\times10^{22}$, $F = 0.96\times10^{5}\,\mathrm{C\,M^{-1}}$, $k = 1.38\times10^{-23}\,\mathrm{J\,K^{-1}}$.

Applying the above numeric values and relations (6) and (6.1) and solving the system (12.1)–(12.4) result in relation (13) for FC current density j_{FC}:

$$j_{\mathrm{FC}} = (42\times10^{3}C_{\mathrm{C}}^{\mathrm{water}} - 488)\,\mathrm{A\,m^{-2}} \tag{13}$$

The current density has the highest value if water concentration $C_{\mathrm{C}}^{\mathrm{water}}$ is the highest. If considering operation without flooding, $C_{\mathrm{C}}^{\mathrm{water}} \leq C_{\mathrm{sat}}^{\mathrm{water}}$. The limiting current density for fuel cell, which

operates without flooding, $\lim j_{FC}^{NOflooding}$, may be assessed by substitution of C_{sat}^{water} for C_C^{water} in Eq. (13):

$$\lim j_{FC}^{NOflooding} \cong 480\ A\ m^{-2} \tag{14}$$

Such impractically low value may be explained by the fact that room temperature values were used. As a rule, PEM fuel cell operational temperatures are commonly in a range of 60–80 °C; insertion of C_{sat}^{water} for 80 °C ($\sim 290 \times 10^{-3}$ kg m^{-3}) into Eq. (13) gives the value $\sim 1.2 \times 10^4$ A m^{-2} for limiting current density (instead of 0.05×10^4 A m^{-2}). The limiting current density is expected to be even higher in case of elevated temperatures, since water diffusion coefficients and mass transfer coefficients increase with the temperature. Also, usually some water vapor super saturation takes place in course of PEM FC, which may increase C_C^{water} over C_{sat}^{water} value; this effect increases limiting current even more.

4. PEM FC unit modifications and assessment of flooding limits of modified PEM FC units

4.1. PEM FC unit with water-sealed cathode compartment

As it may be seen from relations (12.1) and (12.3), water flux through anode GDL toward anode gas channel may substantially exceed water flux through cathode GDL toward cathode gas channel if the difference $C_D^{water} - \langle \hat{C}_{CChannel}^{water} \rangle$ at the cathode side of the FC is equal to the difference $C_A^{water} - \langle C_{AChannel}^{water} \rangle$ at the anode side of the FC. It may be explained by the fast water diffusion in hydrogen, comparing with the water diffusion in air/oxygen; combining (4), (4.1), (6), (6.1) gives the following relation between $\hat{J}_{CChannel}^{water}$ and $J_{AChannel}^{water}$:

$$\frac{J_{AChannel}^{water}}{\hat{J}_{CChannel}^{water}} = \frac{D_{hydrogen}^{air}}{D_{air}^{hydrogen}} = \frac{0.9 \times 10^{-4}\ m^2\ s^{-1}}{0.26 \times 10^{-4}\ m^2\ s^{-1}} \cong 3.5 \tag{15}$$

The circumstance hints that it may be advantageous, from the flooding point of view, to redirect all water vapor flux into the hydrogen channel. The additional benefits may be expected in this case because of the possible alleviation of the insufficient wetting of near-anode PEM layer [13,14]. Also, there are some design-related benefits of anode water removal [15].

Seemingly direct way to achieve FC operation with anode water removal is locking up water vapors in a cathode GBL (or in a shell, which surrounds the cathode compartment and which material is water proof but air permeable) and operating the cell in the dead-ended mode (if substantially pure oxygen is employed as the oxidant supply) or in the low oxygen stoichiometry mode (if air is employed). In this case, the generated water is retained inside cathode compartment, which suggests that an elevated water vapor concentration builds up at a cathode side of PEM ($C_{CChannel}^{water}$ or C_{shell}^{water}), eventually $C_{shell}^{water} = C_{sat}^{water}$, and the concentration gradient is supposed to drive water back trough PEM toward the anode gas channel [16,17].

The above design may be described by Eqs. (16.1)–(16.3), which are, in essence, the modified system (12.1)–(12.4), when $C_C^{water} = C_D^{water} = \hat{C}_{CChannel}^{water}$:

$$\frac{M^{water}}{F}\left(\frac{1+2\alpha}{2}\right)\tilde{j}_{FC} = D_{PEM}^{water}\frac{C_C^{water} - C_B^{water}}{\delta_{PEM}} \tag{16.1}$$

$$D_{hydrogen}^{water}\varepsilon\frac{C_B^{water} - C_A^{water}}{\delta_{GDL}} = h_m(C_A^{water} - \langle C_{AChannel}^{water} \rangle) \tag{16.2}$$

$$\frac{M^{water}}{2F}\tilde{j}_{FC} = h_m(C_A^{water} - \langle C_{AChannel}^{water} \rangle) \tag{16.3}$$

For sake of comparison, it is natural to use the numerical values $i \div x$ for diffusion coefficients, mass transfer coefficients and transference numbers, etc., for numerical estimate of the limiting current density in case of anode water removal. The assessment of the maximal pre-flooding current (the current, which may be reached in case of $C_C^{water} = C_{sat}^{water}$) gives the value (17):

$$\lim \tilde{j}_{FC}^{NOflooding} \cong 0.7\ A\ m^{-2} \tag{17}$$

Such a small value is impractical; the value is so small because of slow water vapor diffusion through Nafion™.

4.2. PEM FC unit with oxygen permeable/water impermeable cathode

It is known that, in case of Nafion™ 117, it takes on the order of 100–1000 s for the membrane to be hydrated when equilibrated with water vapors, and only about 20 s for getting to 80% of its equilibrium water content when it is immersed into liquid water. This fact suggests that PEM water vapor transport kinetics is strongly influenced by water vapor absorbance processes at the Nafion™ interface [18].

From this point of view, attempts to divert a water flow from cathode channel by transporting cathode-born liquid water through PEM under capillary pressure may be worth to be considered [19,20]. There may be a problem from the point of a practical design though, since the capillary, which have to be filled with water for pressure buildup, belong to cathode GDL and thus are also used for the air/oxygen delivery towards catalyst cathode layer.

It may be more promising to divert the water flow from cathode channel by impregnating the cathode structure with water-immiscible but oxygen permeable substance [21]; liquid perfluorocarbones (PFC) are particular examples of such substances (e.g. perfluorooctane and perfluorohexyloctane). The following consideration of the Nafion™ membrane/PFC interface structure helps to understand a physical nature of operation of these cathodes. The calculations, which are presented below, make a rough estimate of potentialities of such a design.

Nafion™ membrane comprises of hydrophobic reticulated structure and percolated hydrophilic regions; in case of hydrated membrane these regions are filled with water [22,23]. Typical pattern of such Nafion™ systems are shown in Fig. 4. The model of the Nafion™ surface, which is presented in Fig. 5,

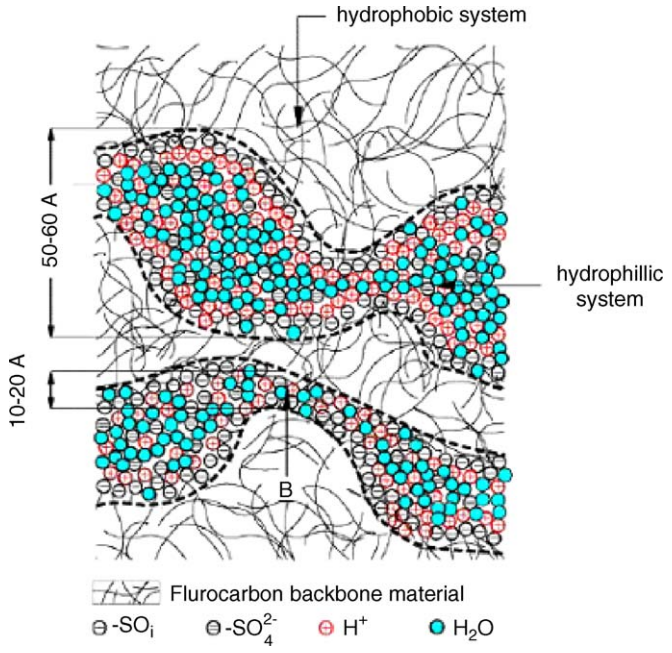

Fig. 4. Nafion^{TM} cluster network model [24].

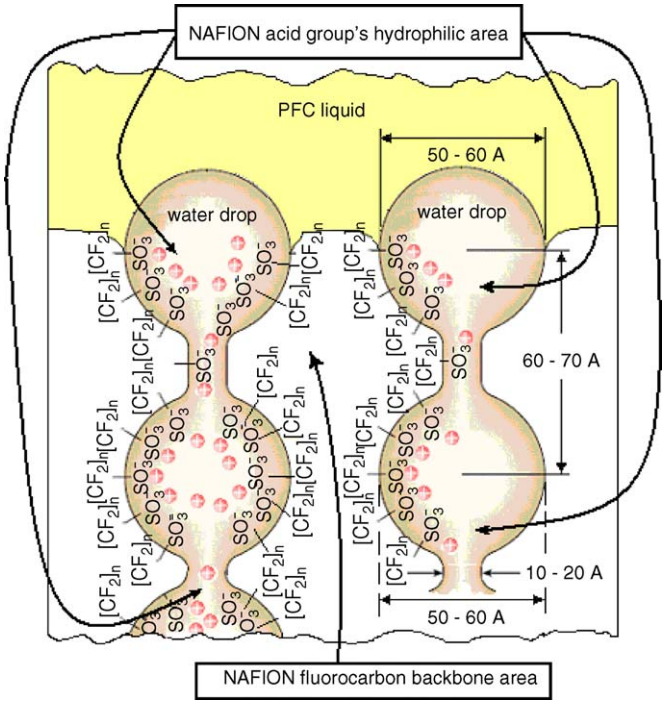

Fig. 5. Schematic representation of Nafion^{TM}/[PFC liquid] interface.

takes into consideration the immiscibility of PFC liquid and water, and also the hydrophobic nature of Nafion^{TM}–air surface (water contact angle at a Nafion^{TM}–air border $\theta > 75^\circ$ [24]; it has to be taken into account that this is a kind of averaged macroscopic value, which is the result of averaging microscopic contact angle values on hydrophilic water-filled pore areas and contact angle values on hydrophobic fluorinated backbone areas). The model suggests that Nafion^{TM} membrane presents water-filled capillary system when borders with PFC liquid. The capillary pressure Δp_b^a in a capillary filled with liquid 'a' and bordering with media 'b' (see Fig. 6) may be calculated according to the Young–Laplace Eq. (18) for the pressure drop across a curved interface, taking into consideration that the meniscus (interface) in a small circular, liquid-filled capillary tube is a hemisphere and the principal radius of curvature is r_i and σ_b^a is a surface tension at the a/b interface:

$$\Delta p_b^a = \sigma_b^a \frac{1}{r_i}. \tag{18}$$

The pressure drop across Nafion^{TM} PEM, which is sandwiched between hydrogen-filled anode GDL and PFC-liquid filled cathode GDL, is governed by relation (19):

$$\Delta p_{PEM} = \sigma_{PFC}^{water} \frac{1}{r_{PFC}^{water}} - \sigma_{hydrogen}^{water} \frac{1}{r_{hydrogen}^{water}}. \tag{19}$$

It is essential that $r_{hydrogen}^{water}, r_{PFC}^{water} \geq r_{pore}^{Nafion}$.

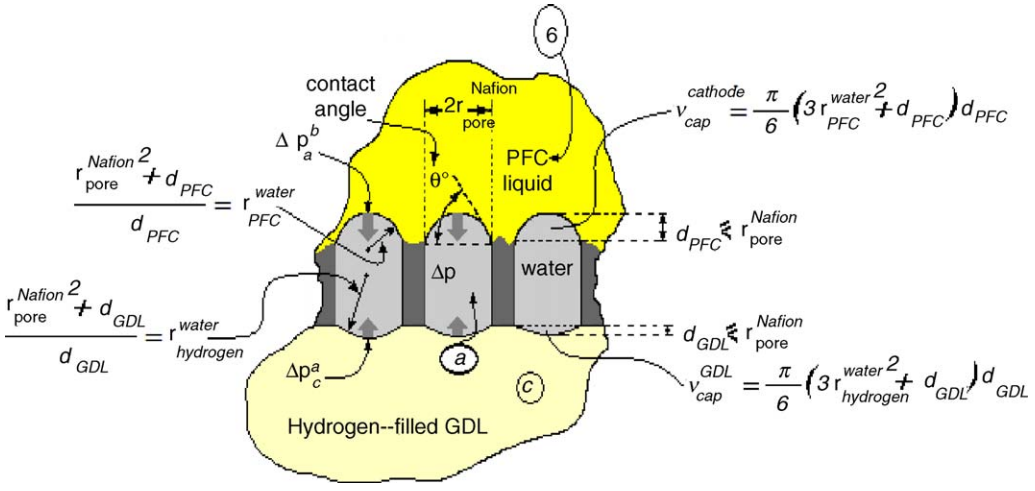

Fig. 6. Capillary pressure inside PEM.

Considering Nafion™ as porous media, the water flux trough PEM $\mathrm{pfc}J^{\mathrm{water}}_{\mathrm{PEM}}$ is governed by Darcy's law:

$$\begin{aligned}&\mathrm{pfc}J^{\mathrm{water}}_{\mathrm{PEM}}\\&= \rho_{\mathrm{water}} \times u = \rho_{\mathrm{water}} \frac{k_p}{\mu^{\mathrm{water}}_{\mathrm{Nafion}}} \nabla p = \rho_{\mathrm{water}} \frac{k_p}{\mu^{\mathrm{water}}_{\mathrm{Nafion}}} \frac{\Delta p_{\mathrm{PEM}}}{\delta_{\mathrm{PEM}}}\\&= \frac{\rho_{\mathrm{water}}}{\sigma_{\mathrm{PEM}}} \frac{k_p}{\mu^{\mathrm{water}}_{\mathrm{Nafion}}} \times \left(\sigma^{\mathrm{water}}_{\mathrm{PFC}} \frac{1}{r^{\mathrm{water}}_{\mathrm{PFC}}} - \sigma^{\mathrm{water}}_{\mathrm{hydrogen}} \frac{1}{r^{\mathrm{water}}_{\mathrm{hydrogen}}} \right);\end{aligned} \tag{20}$$

where u is water flux velocity, ρ_{water} the water density, $\mu^{\mathrm{water}}_{\mathrm{Nafion}}$ the water viscosity in the membrane and k_p is PEM hydraulic permeability.

The water impermeability of cathode layer results in modification of Eqs. (10) and (11):

$$\mathrm{pfc}J^{\mathrm{water}}_{\mathrm{C}} = -\mathrm{pfc}J^{\mathrm{water}}_{\mathrm{PEM}} - J^{\mathrm{water}}_{\mathrm{EOsmos}} + J^{\mathrm{water}}_{\mathrm{Faraday}} \tag{10.1}$$

$$J^{\mathrm{water}}_{\mathrm{AChannel}} = J^{\mathrm{water}}_{\mathrm{Faraday}} \tag{11.1}$$

Combining expressions (2)–(4), (7), (8), (20), (10.1) and (11.1) results in equation system (21.1)–(21.3), which describes water transport in FC unit with PFC-filled cathode:

$$\begin{aligned}&\frac{M^{\mathrm{water}}}{F} \left(\frac{1+2\alpha}{2} \right) \mathrm{pfc}\, j_{\mathrm{FC}}\\&= \mathrm{pfc}J^{\mathrm{water}}_{\mathrm{PEM}} = \rho_{\mathrm{water}} \frac{k_p}{\mu^{\mathrm{water}}_{\mathrm{Nafion}}} \frac{\Delta p_{\mathrm{PEM}}}{\delta_{\mathrm{PEM}}}\end{aligned} \tag{21.1}$$

$$\begin{aligned}&D^{\mathrm{water}}_{\mathrm{hydrogen}} \varepsilon \frac{C^{\mathrm{water}}_{\mathrm{B}} - C^{\mathrm{water}}_{\mathrm{A}}}{\delta_{\mathrm{GDL}}}\\&= \mathrm{pfc}J^{\mathrm{water}}_{\mathrm{GDL}} = h_{\mathrm{m}}(C^{\mathrm{water}}_{\mathrm{A}} - \langle C^{\mathrm{water}}_{\mathrm{AChannel}} \rangle) = \mathrm{pfc}J^{\mathrm{water}}_{\mathrm{AChannel}}\end{aligned} \tag{21.2}$$

$$\frac{M^{\mathrm{water}}}{2F} \mathrm{pfc}\, j_{\mathrm{FC}} = h_{\mathrm{m}}(C^{\mathrm{water}}_{\mathrm{A}} - \langle C^{\mathrm{water}}_{\mathrm{AChannel}} \rangle) = \mathrm{pfc}J^{\mathrm{water}}_{\mathrm{AChannel}} \tag{21.3}$$

$\mathrm{pfc}J^{\mathrm{water}}_{\mathrm{PEM}}$ is equal to zero in stand-by mode (no water production), which means that the pressure drop across PEM also equals zero, and hence $r^{\mathrm{water}}_{\mathrm{hydrogen}} = (\sigma^{\mathrm{water}}_{\mathrm{hydrogen}}/\sigma^{\mathrm{water}}_{\mathrm{PFC}}) r^{\mathrm{water}}_{\mathrm{PFC}}$. When the water production begins, the water "caps" at the cathode PEM side grow and their volume $v^{\mathrm{cathode}}_{\mathrm{cap}}$ increases (see Fig. 5). Equation system (22) below

$$\left\{ \begin{aligned} v^{\mathrm{cathode}}_{\mathrm{cap}} &= \frac{\pi}{6}((3r^{\mathrm{water}}_{\mathrm{PFC}})^2 + d^2_{\mathrm{PFC}}) d_{\mathrm{PFC}} \\ r^{\mathrm{water}}_{\mathrm{PFC}} &= \frac{(r^{\mathrm{Nafion}}_{\mathrm{pore}})^2 + d^2_{\mathrm{PFC}}}{d_{\mathrm{PFC}}} \end{aligned} \right\} \tag{22}$$

reveals that radius $r^{\mathrm{water}}_{\mathrm{PFC}}$ shrinks down along with the $v^{\mathrm{cathode}}_{\mathrm{cap}}$ increase, and that the minimum value of $r^{\mathrm{water}}_{\mathrm{PFC}}$ is $r^{\mathrm{Nafion}}_{\mathrm{pore}}$ (the determination of d_{PFC} is shown in Fig. 6).

In the same way, water transport from GDL/PEM border toward anode gas channel results in decreasing $v^{\mathrm{GDL}}_{\mathrm{cap}}$ and increasing $r^{\mathrm{water}}_{\mathrm{hydrogen}}$. Thus the pressure drop across Nafion™ PEM builds up and hence the water flux across PEM increases along with water production. The maximal value of $^{\mathrm{pfc}}_{\mathrm{lim}}J^{\mathrm{water}}_{\mathrm{PEM}}$ can be assessed from Eq. (20) assuming that Δp_{PEM} reaches its maximal value (Δp_{PEM} peaks at $r^{\mathrm{water}}_{\mathrm{PFC}} = r^{\mathrm{Nafion}}_{\mathrm{pore}}$ and $r^{\mathrm{water}}_{\mathrm{hydrogen}} = \infty$, i.e. water surface is flat at the capillary ends, which are adjacent to GDL). The rough numeric assessment of $^{\mathrm{pfc}}_{\mathrm{lim}}J^{\mathrm{water}}_{\mathrm{PEM}}$ can be performed by using the following numeric parameters: $\mu^{\mathrm{water}}_{\mathrm{Nafion}} = 3.6 \times 10^{-4}$ Pa s [25], $k_p = 1.5 \times 10^{-20}$ m^2 [26], $\delta_{\mathrm{PEM}} = \delta_{\mathrm{Nafion\_112}} = 5 \times 10^{-5}$ m, $\rho_{\mathrm{water}} = 10^3$ kg m^{-3}, $\sigma^{\mathrm{water}}_{\mathrm{PFC}} = 54 \times 10^{-3}$ N m^{-1} [27] and $r^{\mathrm{pore}}_{\mathrm{Nafion}} = 3 \times 10^{-9}$m [24,25]. The assessment gives the value of

$$^{\mathrm{pfc}}_{\mathrm{lim}}J^{\mathrm{water}}_{\mathrm{PEM}} = 1.5 \times 10^{-2}\,\mathrm{kg\,m^{-2}\,s^{-1}}. \tag{23}$$

The rough numeric assessment of maximal values of $\mathrm{pfc}J^{\mathrm{water}}_{\mathrm{GDL}}$ and $\mathrm{pfc}J^{\mathrm{water}}_{\mathrm{AChannel}}$ using numerical values ($i \div x$) gives the following estimate:

$$^{\mathrm{pfc}}_{\mathrm{lim}}J^{\mathrm{water}}_{\mathrm{GDL}} = 4.1 \times 10^{-3}\,\mathrm{kg\,m^{-2}\,s^{-1}} \tag{24}$$

$$^{\mathrm{pfc}}_{\mathrm{lim}}J^{\mathrm{water}}_{\mathrm{AChannel}} = 4.0 \times 10^{-3}\,\mathrm{kg\,m^{-2}\,s^{-1}}, \tag{25}$$

The values for $^{\mathrm{pfc}}_{\mathrm{lim}}J^{\mathrm{water}}_{\mathrm{GDL}}$ and $^{\mathrm{pfc}}_{\mathrm{lim}}J^{\mathrm{water}}_{\mathrm{AChannel}}$ are close and are nearly four times less then $^{\mathrm{pfc}}_{\mathrm{lim}}J^{\mathrm{water}}_{\mathrm{PEM}}$, which reveals that in case under consideration water crossover through PEM may be not a rate determining step. Also, the estimated currents turn to be fairly high (value of $^{\mathrm{pfc}}_{\mathrm{lim}}J^{\mathrm{water}}_{\mathrm{PEM}}$ corresponds to the current $\sim 16 \times 10^4$ A m^{-2}, and values of $^{\mathrm{pfc}}_{\mathrm{lim}}J^{\mathrm{water}}_{\mathrm{GDL}}$ and $^{\mathrm{pfc}}_{\mathrm{lim}}J^{\mathrm{water}}_{\mathrm{AChannel}}$ correspond to the current $\sim 4.2 \times 10^4$ A m^{-2}). It suggests that this design may keep all aforementioned advantages of removing water from anode side of PEM FC unit and also provide means to attain a significantly high FC unit current density.

5. Conclusions

The above assessment of water transport phenomena of a practical PEM FC demonstrates that water transport issues essentially constrain its performance. A new scheme of water management, which is based on redirection of water fluxes toward anode compartment, has been presented. According to this water management scheme, FC cathode structure is impregnated with oxygen permeable-water vapors impermeable substances; typical examples of such substances are perfluorinated hydrocarbons. The numerical assessment demonstrates that this water management scheme may offer a substantial improvement of PEM FC performance.

References

[1] M. Roelofs, DuPont Fuel Cells, NSF Workshop Arlington, Virginia, November 14, 2001.
[2] E.H. Sanders, K.A. McGrady, G.E. Wnek, C.A. Edmondson, J.M. Mueller, J.J. Fontanella, S. Suarez, S.G. Greenbaum, J. Power Sources 129 (2004) 55–61.
[3] P. Berg, K. Promislow, J. St. Pierre, J. Stumper, B. Wetton, J. Electrochem. Soc. 151 (2004) A341–A353.

[4] U. Pasaogullari, C.Y. Wang, J. Electrochem. Soc. 151 (2004) A399–A406.
[5] D.M. Bernardi, M.W. Verbrugge, J. Electrochem. Soc. 139 (9) (1992) 2477–2491.
[6] Z.H. Wang, C.Y. Wang, K.S. Chen, J. Power Sources 94 (2001) 40–50.
[7] T. Okada, G. Xie, Y. Tanabe, J. Electroanal. Chem. 413 (1996) 49–65.
[8] T.A. Zawodzinski, M. Neeman, L.O. Sillerud, S. Gottesfeld, J. Phys. Chem. 95 (1991) 6040–6044.
[9] T.A. Zawodzinski, J. Dawy, J. Valerio, S. Gottesfeld, Electrochim. Acta 40 (1995) 297–302.
[10] http://www.dupont.com/fuelcells/pdf/nae101.pdf.
[11] J.S. Yi, T. Van Nguyen, J. Electrochem. Soc. 146 (1999) 38–45.
[12] A.N. Berezhnoi, A.V. Semenov, Binary Diffusion Coefficients of Liquid Vapors in Gases, Begell House, 1997, p. 61.
[13] B. Andreaus, G.G. Scherer, Solid State Ionics 168 (2004) 311–320.
[14] T. Okada, G. Xie, Y. Tanabe, J. Electroanal. Chem. 413 (1996) 49–65.
[15] H.H. Voss, D.P. Wilkinson, P.G. Pickup, M.C. Johnson, V. Basura, Electrochim. Acta. 40 (1995) 321–328.
[16] D.P. Wilkinson, H.H. Voss, D.S. Watkins, K.B. Prater, US Patent 5,366, 818.
[17] E. Peled, T. Duvdevani, A. Blum, V. Livshits, A. Aharon, US Patent Application 20040209153.
[18] S. Ge, X. Li, B. Yi, I.-M. Hsing, J. Electrochem. Soc. 152 (2005) A1149–A1157.
[19] X. Ren, J.J. Becerra, R.S. Hirsch, S. Gottesfeld, F.W. Kovacs, K.J. Shufon, US Patent Application 20040209136.
[20] X. Ren, F.W. Kovacs, K.J. Shufon, S. Gottesfeld, US Patent Application 20040209154.
[21] S.A. Grot, US Patent 6,740,445.
[22] Q. Li, R. He, J.O. Jensen, N.J. Bjerrum, Chem. Mater. 15 (2003) 4896–4915.
[23] K.D. Kreuer, J. Membr. Sci. 185 (2001) 29–39.
[24] H.-P. Brack, M. Slaski, L. Gubler, G.G. Scherer, S. Alkan, A. Wokaun, Fuel Cells 4 (2004) 141–146.
[25] G.H. Guvelioglu, H.G. Stenger, J. Power Sources 147 (1–2) (2005) 95–106.
[26] F. Meier, G. Eigenberger, Electrochim. Acta 49 (2004) 1731–1742.
[27] Medicel AG (Switzerland), Product Information: F-OctanePLUS, Interface Tension, http://www.medicelag.com/products/download/7_7/774.pdf.